AIMS Mathematics, 9(3): 7627–7644.
DOI: 10.3934/math.2024370
Received: 29 December 2023
Revised: 29 January 2024
Accepted: 04 February 2024
Published: 22 February 2024

http://www.aimspress.com/journal/Math

Research article

Quasi-projective and finite-time synchronization of fractional-order memristive complex-valued delay neural networks via hybrid control

Jiaqing Zhu[1], **Guodong Zhang**[1,*] **and Leimin Wang**[2]

[1] College of Mathematics and statistics, South-Central Minzu University, Wuhan 430074, China
[2] School of Automation, China University of Geosciences, Wuhan 430074, China

* **Correspondence:** Email: zgd2008@mail.scuec.edu.cn.

Abstract: We focused on the quasi-projective synchronization (QPS) and finite-time synchronization (FNTS) for a class of fractional-order memristive complex-valued delay neural networks (FOMCVDNNs). Rather than decomposing the complex-valued system into its real and imaginary components, we adopted a more streamlined approach by introducing a lemma associated with the complex-valued sign function. This innovative technique enabled us to design a simpler discontinuous controller. Then, based on the finite-time Lemma, measurable selection theorem, Lyapunov function theory, properties of the Mittag-Leffler function, and the fractional-order Razumikhin theorem, various substantial results were derived using a novel hybrid control scheme. In conclusion, we presented numerical simulations to illustrate the practical effectiveness of our theoretical findings.

Keywords: quasi-projective synchronization; finite-time synchronization; fractional-order; complex-valued; hybrid control
Mathematics Subject Classification: 34A08, 34D06, 34K37, 93C23

1. Introduction

In recent decades, neural networks (NNs) have found widespread application across diverse fields, including associative memories, signal and image processing, pattern recognition, and combinatorial optimization [1–4]. Scholars and researchers have closely observed the progress in NNs with great interest.

Incorporating fractional-order dynamics offers a more nuanced portrayal of temporal relationships and memory influences. This enriches the model's capacity to grasp intricate behaviors in practical, real-world scenarios. Moreover, fractional-order exhibit favorable properties in comparison to integer orders, implying that fractional-order approaches can yield results that more accurately reflect real-world phenomena. At present, fractional-order neural networks find widespread application and have

yielded numerous outstanding results [5–7]. The incorporation of memristive elements [8] introduces adaptive and non-linear characteristics, fostering a more biologically inspired approach to neural network modeling. In addition, time delay is inevitable in the transmission of information in neural networks; Thus, so adding time delay to neural networks is more practical [9].

Many practical applications of NNs involve handling complex signals, which are challenges that cannot be effectively addressed by real-valued neural networks (RVNNs). However, complex-valued neural networks (CVNNs) emerge as a promising solution for resolving such intricate problems. CVNNs, equipped with both real and imaginary components, offer a more comprehensive framework for modeling intricate relationships in diverse applications, such as signal processing, image recognition, and communication systems [10–12]. However, the inherent nonlinearity, time delays, and fractional-order dynamics in such networks pose considerable challenges in achieving synchronization, a critical phenomenon in the study of interconnected systems.

QPS, characterized by asymptotic synchronization with an arbitrary scaling factor, provides a versatile framework for controlling the synchronization behavior in complex systems. Furthermore, the focus on FNTS addresses the practical importance of achieving rapid and precise synchronization in various applications. This synchronization technique is often used in secure communication systems, where the transmitter and receiver systems need to synchronize their chaotic dynamics to ensure proper decoding of information. FNTS aims to achieve synchronization between two systems within a predetermined finite time. The synchronization is not only guaranteed but is also achieved in a specified time duration. Moreover, it is particularly relevant in scenarios where time efficiency is critical, such as in secure communication protocols or real-time control systems. Consequently, QPS and FNTS have emerged as prominent areas of exploration, with numerous findings being documented in prior studies [13–19].

Until now, there have been limited synchronization results associated with FOMCVDNNs. To address this gap, we aim to contribute by deriving several novel results to guarantee QPS and FNTS through a hybrid adaptive control approach. The integration of fractional calculus, memristive devices, and time delays in neural network models enhances their capacity to accurately capture the underlying dynamics of real-world systems. Our results not only contribute to the theoretical understanding of complex neural network synchronization but also pave the way for practical applications in diverse fields. The primary contributions in this context can be encapsulated through the following dimensions:

(1) Traditional approaches, as highlighted in prior works [20–23], have typically analyzed complex-valued systems by decomposing them into real and imaginary components. In contrast, our innovative methodology introduces complex-valued sign functions and utilizes non-separation techniques to tackle FOMCVDNNs.

(2) Compared with the sliding mode control [21], quantized control [24], and adaptive control [25], we use hybrid adaptive control to get QPS and FNTS of FOMCVDNNs.

The remainder of the paper is organized as follows: Section 2 provides a concise overview of mathematical prerequisites, encompassing fractional-order calculus, QPS, and FNTS Lemma. Additionally, the FOMCVDNNs model is introduced. The major results and analysis are presented in Section 3, followed by numerical simulations in Section 4 to validate the theoretical findings. In conclusion, Section 5 wraps up the paper by exploring potential applications and suggesting directions for future research. The symbols used in this paper are shown in Table 1.

Table 1. The meaning of symbols in the article.

Notation	Meaning
$\mathbb{R}$	real number domains
$\mathbb{C}$	complex number domains
$\mathbb{Q}$	natural number set
$\mathbf{i}$	imaginary unit and $\sqrt{-1} = \mathbf{i}$
$\overline{u}$	conjugation of u, $u = a + b\mathbf{i} \in \mathbb{C}$, $\overline{u} = a - b\mathbf{i}$
$Re(u)$	the real part of u
$Im(u)$	the imag part of u
$\overline{co}[\alpha^*, \alpha^{**}]$	the convex hull of $\{\alpha^*, \alpha^{**}\}$
$[u]$	$sign(Re(u)) + \mathbf{i}sign(Im(u))$
$\|u\|_1$	$\|Re(u)\| + \|Im(u)\|$
$\|u\|_2$	$\sqrt{\overline{u}u}$
$\varsigma_{\iota\jmath}(t)$	$max\{\|\varsigma_{\iota\jmath}^*\|_1, \|\varsigma_{\iota\jmath}^{**}\|_1\}$
$\sigma_{\iota\jmath}(t)$	$max\{\|\sigma_{\iota\jmath}^*\|_1, \|\sigma_{\iota\jmath}^{**}\|_1\}$
Ω_i	the switching jump
$\beth_\jmath(\cdot)$, $\daleth_\jmath(\cdot)$	complex-valued activation function
τ	$\tau = max\{\tau(t)\}$
$I_\iota(t)$	external input

2. Preliminaries and model description

In this segment, we will provide an overview of QTS and FTS. Additionally, we will introduce a selection of crucial lemmas and definitions that will play a pivotal role in the forthcoming mathematical derivations.

Definition 2.1. [26] The Caputo derivation in κ-order for the function $\Theta(t)$ is defined as

$$ {}_{t_0}D_t^{\kappa}\Theta(t) = \frac{1}{\Gamma(\gamma-\kappa)}\int_{t_0}^{t}(t-\pi)^{\gamma-\kappa-1}\Theta^{\gamma}(\pi)d\pi, $$

where γ represents a positive integer, $\gamma - 1 < \kappa < \gamma$, t_0 is the initial time, $\Gamma(\gamma) = \int_0^\infty \pi^{\gamma-1}e^{-\pi}d\pi$ is the Gamma function.

Definition 2.2. The beta function, denoted as $B(\alpha,\beta)$, is a mathematical function defined when $\alpha,\beta \in \mathbb{R}^+$:

$$ B(\alpha,\beta) = \int_0^1 \upsilon^{\alpha-1}(1-\upsilon)^{\beta-1}d\upsilon. $$

Definition 2.3. [26] When considering a parameter $\kappa > 0$ and $\chi \in \mathbb{C}$, the Mittag-Leffler function can be characterized as follows:

$$ E_\kappa(\chi) = \sum_{\iota=0}^{+\infty}\frac{\chi^\iota}{\Gamma(\kappa\iota+1)}. $$

Definition 2.4. [14] FOMCVDNNs (2) and FOMCVDNNs (3) are deemed to achieve QPS if there exist a small error bound ϵ such that $\lim_{t\to\infty} \|\Psi_\iota(t) - \hbar\Phi_\iota(t)\|_p \leq \epsilon, p = 1, 2$. Here the symbol $\hbar$ denotes a projective coefficient belonging to $\mathbb{R}$.

Definition 2.5. [27] FOMCVDNNs (2) and (3) are deemed to achieve FNTS through designing a hybrid controller, if there exists $t > 0$ such that $\lim_{t\to T} \|\Upsilon(t)\| = 0$ and $\|\Upsilon(t)\| \equiv 0$ for $\forall t > T$, T is called the settling time of synchronization.

Lemma 2.1. [28] For any given $\emptyset(t) \in \mathbb{C}$, the following equation remains valid:

$$(1)\ \overline{\emptyset(t)}[\emptyset(t)] + \emptyset(t)[\overline{\emptyset(t)}] = 2|\emptyset(t)|_1 \geq 2|\emptyset(t)|_2.$$
$$(2)\ 0 < \kappa < 1, D^\kappa|\emptyset(t)|_1 \leq \frac{1}{2}([\overline{\emptyset(t)}]D^\kappa\emptyset(t) + [\emptyset(t)]D^\kappa\overline{\emptyset(t)}).$$
$$(3)\ [\overline{\emptyset(t)}][\emptyset(t)] = |[\emptyset(t)]|_1.$$

Lemma 2.2. [28] For any $\emptyset(t) \in \mathbb{C}$ and any measurable selection $\partial(t) \in \overline{co}([\emptyset(t)])$, where

$$\overline{co}([\emptyset(t)]) = \overline{co}(sign(Re(\emptyset(t)))) + \mathbf{i}\overline{co}(sign(Im(\emptyset(t)))).$$

The following equation remains valid:

$$[\overline{\emptyset(t)}]\partial(t) + \overline{\partial(t)}[\emptyset(t)] = 2|\emptyset(t)|_1,$$
$$\overline{\emptyset(t)}\partial(t) + \overline{\partial(t)}\emptyset(t) = 2|\emptyset(t)|_1 \geq 2|\emptyset(t)|_2.$$

Lemma 2.3. [29] For $\chi_\iota \geq 0$ where $\iota \in \mathbb{Q}$, and given that $0 < \mu \leq 1$, and $\nu > 1$, we can express this as

$$\sum_{\iota=1}^{n} \chi_\iota^\mu \geq (\sum_{\iota=1}^{n} \chi_\iota)^\mu, \quad \sum_{\iota=1}^{n} \chi_\iota^\nu \geq n^{1-\nu}(\sum_{\iota=1}^{n} \chi_\iota)^\nu.$$

Lemma 2.4. [30] Assuming a continuous and non-negative function denoted as $\mathbb{V}(t)$, considering that

$$D^\kappa\mathbb{V}(t) \leq -\psi\mathbb{V}(t)^\zeta, \mathbb{V}(t) \in \mathbb{R}_+\backslash\{0\}, \tag{1}$$

where $t \geq 0$, $\psi > 0$ and $0 \leq \zeta < \kappa < 1$, then $\lim_{t\to T} \mathbb{V}(t) = 0$ and $\mathbb{V}(t) \equiv 0$ for $t \geq T$, in which $T = t_0 + (\frac{\kappa}{\psi}\mathbb{V}^{\kappa-\zeta}(t_0)B(\kappa, 1-\zeta))^{\frac{1}{\kappa}}$.

Lemma 2.5. [14] Provided a non-negative continuous function $\chi(t)$ that adheres to the inequality:

$${}_{t_0}D_t^\kappa \leq -\varpi\chi(t) + \varrho,$$

where $0 < \kappa < 1$, $\varpi > 0$ and $\varrho > 0$. then, for any $t > t_0$ we can express it as:

$$\chi(t) \leq (\chi(t_0) - \frac{\varrho}{\varpi})E_\kappa(-\varpi(t-t_0)^\kappa) + \frac{\varrho}{\varpi}.$$

Lemma 2.6. [31] The expression $E_\kappa(\varpi(t-t_0)^\kappa)$ is monotonically non-increasing for $t > t_0$, and it satisfies the inequality $0 \leq E_\kappa(\varpi(t-t_0)^\kappa) \leq 1$ and $\lim_{t\to+\infty} E_\kappa(\varpi(t-t_0)^\kappa) = 0$ whenever $\varpi \leq 0$.

In this paper, a class of FOMCVDNNs is given as

$$\begin{cases} {}_{t_0}D_t^{\kappa}\Phi_\iota(t) = -o_\iota\Phi_\iota(t) + \sum\limits_{\jmath=1}^{n} \varsigma_{\iota\jmath}(\Phi_\iota(t))\beth_\jmath(\Phi_\jmath(t)) + \sum\limits_{\jmath=1}^{n} \sigma_{\iota\jmath}(\Phi_\iota(t))\daleth_\jmath(\Phi_\jmath(t-\tau(t))) + I_\iota(t), \\ \Phi_\iota(\upsilon) = \dagger_\iota(\upsilon) \in \mathbb{C}, \upsilon \in [-\tau, t_0], \end{cases} \tag{2}$$

where $0 < \kappa < 1$, $\iota \in \mathbb{Q}$, $\Phi_\iota(t) \in \mathbb{C}$ represent the state of the ι-th neuron at time t. The parameter $o_\iota \in \mathbb{R}$ signifies the rate at which a neuron inhibits itself, where $o_\iota > 0$. $\varsigma_{\iota\jmath}(\Phi_\iota(t))$ and $\sigma_{\iota\jmath}(\Phi_\iota(t))$ can be alternatively described as the neural network connection parameter and the time-delayed neural network connection parameter, respectively; $\tau(t)$ denotes time delay about t; Let's denote $\beth_\jmath(\cdot)$ and $\daleth_\jmath(\cdot)$ as complex-valued activation functions for the $\jmath$th neuron at time t and $t-\tau(t)$, respectively; $I_\iota(t) \in \mathbb{C}$ represents the external input; $\Phi_\iota(\upsilon) = \dagger_\iota(\upsilon)$ is the initial condition of FOMCVDNNs (2). The parameters $\varsigma_{\iota\jmath}(\Phi_\iota(t))$, $\sigma_{\iota\jmath}(\Phi_\iota(t))$ are state-dependent and satisfy

$$\varsigma_{\iota\jmath}(\Phi_\iota(t)) = \begin{cases} \varsigma_{\iota\jmath}^{*}, & |\Phi_\iota(t)|_1 \le \Omega_\iota \\ \varsigma_{\iota\jmath}^{**}, & |\Phi_\iota(t)|_1 > \Omega_\iota \end{cases} \qquad \sigma_{\iota\jmath}(\Phi_\iota(t)) = \begin{cases} \sigma_{\iota\jmath}^{*}, & |\Phi_\iota(t)|_1 \le \Omega_\iota \\ \sigma_{\iota\jmath}^{**}, & |\Phi_\iota(t)|_1 > \Omega_\iota \end{cases}$$

where $\varsigma_{\iota\jmath}^{*}, \varsigma_{\iota\jmath}^{**}, \sigma_{\iota\jmath}^{*}, \sigma_{\iota\jmath}^{**}, \iota, \jmath \in \mathbb{Q}$ are complex-valued constants.

Hypothesis 2.1. For every $\jmath \in \mathbb{Q}$, $\ell = 1, 2$ and $u, v \in \mathbb{C}$, there exist positive real constants $\dot{\beth}_{\ell\jmath}$ and $\dot{\daleth}_{\ell\jmath}$, such that

$$|\beth_\jmath(u) - \beth_\jmath(v)|_\ell \le \dot{\beth}_{\ell\jmath}|u-v|_\ell, \qquad |\daleth_\jmath(u) - \daleth_\jmath(v)|_\ell \le \dot{\daleth}_{\ell\jmath}|u-v|_\ell.$$

Hypothesis 2.2. For any complex number π, $\iota, \jmath \in \mathbb{Q}$ and $\ell = 1, 2$, there are positive constants $\eta_{\ell\jmath}$, $\delta_{\ell\jmath}$ and $\varphi_{\ell\iota}$ such that the following inequalities hold:

$$|\beth_\jmath(\pi)|_\ell \le \eta_{\ell\jmath}, \qquad |\daleth_\jmath(\pi)|_\ell \le \delta_{\ell\jmath}, \qquad |I_\iota(t)|_\ell \le \varphi_{\ell\iota}.$$

When referring to the drive system labeled as FOMCVDNNs (2), we can describe its corresponding response system as

$$\begin{cases} {}_{t_0}D_t^{\kappa}\Psi_\iota(t) = -o_\iota\Psi_\iota(t) + \sum\limits_{\jmath=1}^{n} \varsigma_{\iota\jmath}(\Psi_\iota(t))\beth_\jmath(\Psi_\jmath(t)) + \sum\limits_{\jmath=1}^{n} \sigma_{\iota\jmath}(\Psi_\iota(t))\daleth_\jmath(\Psi_\jmath(t-\tau(t))) + u_\iota(t) + I_\iota(t), \\ \Psi_\iota(\upsilon) = \ddagger_\iota(\upsilon) \in \mathbb{C}, \upsilon \in [-\tau, t_0], \end{cases} \tag{3}$$

where $\Psi_\iota(t) \in \mathbb{C}$ is the state variable of FOMCVDNNs (3); $u_\iota(t)$ is the hybrid controller; $\Psi_\iota(\upsilon) = \ddagger_\iota(\upsilon)$ is the initial condition of FOMCVDNNs (3).

We design the hybrid controller $u_\iota(t)$ as followed:

$$u_\iota(t) = -c_\iota\Upsilon_\iota(t) - d_\iota[\Upsilon_\iota(t)] - \nu_\iota(t), \tag{4}$$

where c_ι and d_ι are all positive constants, $\Upsilon_\iota(t) = \Psi_\iota(t) - \hbar\Phi_\iota(t), \hbar \in \mathbb{R}$ is the synchronization error signal and $\nu_\iota(t)$ is designed as follows:

$$\nu_\iota(t) = \begin{cases} 0, |\Phi_\iota(t)|_1 \le \Omega_\iota, |\Psi_\iota(t)|_1 \le \Omega_\iota, \\ 0, |\Phi_\iota(t)|_1 > \Omega_\iota, |\Psi_\iota(t)|_1 > \Omega_\iota, \\ \hbar \sum\limits_{\jmath=1}^{n} \Big[(\varsigma_{\iota\jmath}^{**} - \varsigma_{\iota\jmath}^{*})\beth_\jmath(\Phi_\jmath(t)) + (\sigma_{\iota\jmath}^{**} - \sigma_{\iota\jmath}^{*}) \times \daleth_\jmath(\Phi_\jmath(t-\tau(t)))\Big], |\Phi_\iota(t)|_1 \le \Omega_\iota, |\Psi_\iota(t)|_1 > \Omega_\iota, \\ \hbar \sum\limits_{\jmath=1}^{n} \Big[(\varsigma_{\iota\jmath}^{*} - \varsigma_{\iota\jmath}^{**})\beth_\jmath(\Phi_\jmath(t)) + (\sigma_{\iota\jmath}^{*} - \sigma_{\iota\jmath}^{**}) \times \daleth_\jmath(\Phi_\jmath(t-\tau(t)))\Big], |\Phi_\iota(t)|_1 > \Omega_\iota, |\Psi_\iota(t)|_1 \le \Omega_\iota. \end{cases} \tag{5}$$

From FOMCVDNNs (2) and (3) ,we can get the following error systems by $\Upsilon_\iota(t) = \Psi_\iota(t) - \hbar\Phi_\iota(t)$

$$
\begin{aligned}
{}_{t_0}D_t^{\kappa}\Upsilon_\iota(t) =& -o_\iota\Upsilon_\iota(t) + \sum_{\jmath=1}^{n}\varsigma_{\iota\jmath}(\Psi_\iota(t))\daleth_\jmath(\Psi_\jmath(t)) - \hbar\sum_{\jmath=1}^{n}\varsigma_{\iota\jmath}(\Phi_\iota(t))\daleth_\jmath(\Phi_\jmath(t)) + \sum_{\jmath=1}^{n}\sigma_{\iota\jmath}(\Psi_\iota(t))\beth_\jmath(\Psi_\jmath(t-\tau(t)))\\
&- \hbar\sum_{\jmath=1}^{n}\sigma_{\iota\jmath}(\Phi_\iota(t))\beth_\jmath(\Phi_\jmath(t-\tau(t))) + (1-\hbar)I_\iota(t) + u_\iota(t). \qquad (6)
\end{aligned}
$$

Under the hybrid controller (4), the error system (6) can be covered with the following differential inclusions

$$
\begin{aligned}
{}_{t_0}D_t^{\kappa}\Upsilon_\iota(t) \in& -(o_\iota + c_\iota)\Upsilon_\iota(t) + \sum_{\jmath=1}^{n}\overline{co}[\varsigma_{\iota\jmath}^{*},\varsigma_{\iota\jmath}^{**}]\daleth_\jmath(\Psi_\jmath(t)) - \hbar\sum_{\jmath=1}^{n}\overline{co}[\varsigma_{\iota\jmath}^{*},\varsigma_{\iota\jmath}^{**}]\daleth_\jmath(\Phi_\jmath(t)) + \sum_{\jmath=1}^{n}\overline{co}[\sigma_{\iota\jmath}^{*},\sigma_{\iota\jmath}^{**}]\\
&\times\beth_\jmath(\Psi_\jmath(t-\tau(t))) - \hbar\sum_{\jmath=1}^{n}\overline{co}[\sigma_{\iota\jmath}^{*},\sigma_{\iota\jmath}^{**}]\beth_\jmath(\Phi_\jmath(t-\tau(t))) + (1-\hbar)I_\iota(t) - d_\iota[\Upsilon_\iota(t)]. \qquad (7)
\end{aligned}
$$

By utilizing the concepts outlined in the references [32, 33] and the Lemma 2.1 of [34], we can readily address the error system described in (6) by incorporating it into the differential inclusion presented in (7).

Remark 2.1. Due to the nonexistence of a classical solution for FOMCVDNNS (2) and (3), the solutions for all systems considered herein are approached in the Filippov sense. Assuming Hypothesis 2.1 holds, the existence of a solution for (10) can be assured through the proof processes outlined in [34].

In light of the measurable selection theorem [32, 33], it becomes evident that Eq (7) can be reformulated in a different manner, that is, for $\iota \in \mathbb{Q}$, there exist $\varsigma_{\iota\jmath}(t) \in \overline{co}[\varsigma_{\iota\jmath}^{*},\varsigma_{\iota\jmath}^{**}]$ and $\sigma_{\iota\jmath}(t) \in \overline{co}[\sigma_{\iota\jmath}^{*},\sigma_{\iota\jmath}^{**}]$, such that

$$
\begin{aligned}
{}_{t_0}D_t^{\kappa}\Upsilon_\iota(t) =& -(o_\iota + c_\iota)\Upsilon_\iota(t) + \sum_{\jmath=1}^{n}\varsigma_{\iota\jmath}(t)\daleth_\jmath(\Psi_\jmath(t)) - \hbar\sum_{\jmath=1}^{n}\varsigma_{\iota\jmath}(t)\daleth_\jmath(\Phi_\jmath(t))\\
&+ \sum_{\jmath=1}^{n}\sigma_{\iota\jmath}(t)\beth_\jmath(\Psi_\jmath(t-\tau(t))) - \hbar\sum_{\jmath=1}^{n}\sigma_{\iota\jmath}(t)\beth_\jmath(\Phi_\jmath(t-\tau(t))) + (1-\hbar)I_\iota(t) - d_\iota[\Upsilon_\iota(t)]. \qquad (8)
\end{aligned}
$$

By transforming Eq (8), a new synchronization error system is obtained as follows

$$
\begin{aligned}
{}_{t_0}D_t^{\kappa}\Upsilon_\iota(t) =& -(o_\iota + c_\iota)\Upsilon_\iota(t) + \sum_{\jmath=1}^{n}\varsigma_{\iota\jmath}(t)\widehat{\daleth}_\jmath(\Upsilon_\jmath(t)) + \sum_{\jmath=1}^{n}\varsigma_{\iota\jmath}(t)[\daleth_\jmath(\hbar\Phi_\jmath(t)) - \hbar\daleth_\jmath(\Phi_\jmath(t))] + \sum_{\jmath=1}^{n}\sigma_{\iota\jmath}(t)\\
&\times\widehat{\beth}_\jmath(\Upsilon_\jmath(t-\tau(t))) + \sum_{\jmath=1}^{n}\sigma_{\iota\jmath}(t)[\beth_\jmath(\hbar\Phi_\jmath(t-\tau(t))) - \hbar\beth_\jmath(\Phi_\jmath(t-\tau(t)))] + (1-\hbar)I_\iota(t) - d_\iota[\Upsilon_\iota(t)].
\end{aligned} \qquad (9)
$$

where $\widehat{\daleth}_\jmath(\Upsilon_\jmath(t)) = \daleth_\jmath(\Psi_\jmath(t)) - \daleth_\jmath(\hbar\Phi_\jmath(t))$ and $\widehat{\beth}_\jmath(\Upsilon_\jmath(t-\tau(t))) = \beth_\jmath(\Psi_\jmath(t-\tau(t))) - \beth_\jmath(\hbar\Phi_\jmath(t-\tau(t)))$.

3. Main results

3.1. Quasi-projective synchronization

Theorem 3.1. Based on Hypothesis 2.1 and 2.2, the FOMCVDNNs (2) and (3) get QPS under controller (4) if

$$\mathfrak{R} = \mathfrak{I} - \mathfrak{R}_1 - \wp\mathfrak{R}_2 > 0, \tag{10}$$

where

$$\mathfrak{I} = \min_{\iota\in\mathbb{Q}}\{o_\iota + c_\iota\}, \quad \mathfrak{R}_1 = \max_{\iota\in\mathbb{Q}}\{\sum_{j=1}^{n} \dot{\jmath}_{j1}|\varsigma_{\iota j}|_1\}, \quad \mathfrak{R}_2 = \max_{\iota\in\mathbb{Q}}\{\sum_{j=1}^{n} \dot{\neg}_{j1}|\sigma_{\iota j}|_1\}, \quad \wp > 1.$$

Then the error bound is estimated by $\lim_{t\to\infty}\|\Upsilon_\iota(t)\|_1 \leq \frac{\varrho}{\mathfrak{R}}$, where $\varrho = |1-\hbar|_1\sum_{\iota=1}^{n}\varphi_{1\iota} + (1+|\hbar|_1)\sum_{\iota=1}^{n}\sum_{j=1}^{n}\left(|\varsigma_{\iota j}(t)|_1\eta_{1j} + |\sigma_{\iota j}(t)|_1\delta_{1j}\right) - d_\iota$.

Proof. Constructing the designated Lyapunov function as outlined:

$$\mathbb{V}_1(t) = \sum_{\iota=1}^{n}|\Upsilon_\iota(t)|_1.$$

Based on Lemma 2.1, one has

$$\begin{aligned}
&{}_{t_0}D_t^\kappa\mathbb{V}_1(t)\\
\leq&\frac{1}{2}\sum_{\iota=1}^{n}\Big[[\overline{\Upsilon_p(t)}]_{t_0}D_t^\kappa\Upsilon_\iota(t) + [\Upsilon_p(t)]_{t_0}D_t^\kappa\overline{\Upsilon_\iota(t)}\Big]\\
=&-\frac{1}{2}\sum_{\iota=1}^{n}(o_\iota+c_\iota)\Big[\Upsilon_\iota(t)[\overline{\Upsilon_\iota(t)}] + \overline{\Upsilon_\iota(t)}[\Upsilon_\iota(t)]\Big]\\
&+\frac{1}{2}\sum_{\iota=1}^{n}\sum_{j=1}^{n}\Big[[\overline{\Upsilon_\iota(t)}]\varsigma_{\iota j}(t)\widehat{\jmath}_j(\Upsilon_j(t)) + [\Upsilon_\iota(t)]\overline{\varsigma_{\iota j}(t)\widehat{\jmath}_j(\Upsilon_j(t))}\Big]\\
&+\frac{1}{2}\sum_{\iota=1}^{n}\sum_{j=1}^{n}\Big[[\overline{\Upsilon_\iota(t)}]\varsigma_{\iota j}(t)\jmath_j(\hbar\Phi_j(t)) + [\Upsilon_\iota(t)]\overline{\varsigma_{\iota j}(t)\jmath_j(\hbar\Phi_j(t))}\Big]\\
&-\frac{1}{2}\sum_{\iota=1}^{n}\sum_{j=1}^{n}\Big[[\overline{\Upsilon_\iota(t)}]\varsigma_{\iota j}(t)\hbar\jmath_j(\Phi_j(t)) + [\Upsilon_\iota(t)]\overline{\varsigma_{\iota j}(t)\hbar\jmath_j(\Phi_j(t))}\Big]\\
&+\frac{1}{2}\sum_{\iota=1}^{n}\sum_{j=1}^{n}\Big[[\overline{\Upsilon_\iota(t)}]\sigma_{\iota j}(t)\widehat{\neg}_j(\Upsilon_j(t-\tau(t))) + [\Upsilon_\iota(t)]\overline{\sigma_{\iota j}(t)\widehat{\neg}_j(\Upsilon_j(t-\tau(t)))}\Big]\\
&+\frac{1}{2}\sum_{\iota=1}^{n}\sum_{j=1}^{n}\Big[[\overline{\Upsilon_\iota(t)}]\sigma_{\iota j}(t)\neg_j(\hbar\Phi_j(t-\tau(t))) + [\Upsilon_\iota(t)]\overline{\sigma_{\iota j}(t)\neg_j(\hbar\Phi_j(t-\tau(t)))}\Big]\\
&-\frac{1}{2}\sum_{\iota=1}^{n}\sum_{j=1}^{n}\Big[[\overline{\Upsilon_\iota(t)}]\sigma_{\iota j}(t)\hbar\neg_j(\Phi_j(t-\tau(t))) + [\Upsilon_\iota(t)]\overline{\sigma_{\iota j}(t)\hbar\neg_j(\Phi_j(t-\tau(t)))}\Big]
\end{aligned}$$

$$- \frac{1}{2} d_\iota \sum_{\iota=1}^{n} \Big[[\overline{\Upsilon_\iota(t)}][\Upsilon_\iota(t)] + [\Upsilon_\iota(t)][\overline{\Upsilon_\iota(t)}] \Big]$$
$$+ \frac{1}{2} \sum_{\iota=1}^{n} \Big[[\overline{\Upsilon_\iota(t)}](1-\hbar) I_\iota(t) + [\Upsilon_\iota(t)] \overline{(1-\hbar) I_\iota(t)} \Big]. \tag{11}$$

Applying Lemma 2.1, we can rephrase this as follows:

$$- \frac{1}{2} \sum_{\iota=1}^{n} (o_\iota + c_\iota) \Big[\Upsilon_\iota(t) [\overline{\Upsilon_\iota(t)}] + \overline{\Upsilon_\iota(t)} [\Upsilon_\iota(t)] \Big] = - \sum_{\iota=1}^{n} (o_\iota + c_\iota) |\Upsilon_\iota(t)|_1. \tag{12}$$

It follows from Hypothesis 2.1 and Lemma 2.2 that:

$$\frac{1}{2} \sum_{\iota=1}^{n} \sum_{\jmath=1}^{n} \Big[[\overline{\Upsilon_\iota(t)}] \varsigma_{\iota\jmath}(t) \widehat{\beth}_\jmath(\Upsilon_\iota(t)) + [\Upsilon_\iota(t)] \overline{\varsigma_{\iota\jmath}(t) \widehat{\beth}_\jmath(\Upsilon_\iota(t))} \Big] \leq \sum_{\iota=1}^{n} \sum_{\jmath=1}^{n} |\varsigma_{\iota\jmath}(t) \widehat{\beth}_\jmath(\Upsilon_\iota(t))|_1$$
$$\leq \sum_{\iota=1}^{n} \sum_{\jmath=1}^{n} |\varsigma_{\jmath\iota}(t)|_1 \dot{\beth}_{\jmath 1} |\Upsilon_\iota(t)|_1. \tag{13}$$

By invoking Lemma 2.1 and considering Hypothesis 2.2, we obtain

$$\frac{1}{2} \sum_{\iota=1}^{n} \sum_{\jmath=1}^{n} \Big[[\overline{\Upsilon_\iota(t)}] \varsigma_{\iota\jmath}(t) \beth_\jmath(\hbar \Phi_\jmath(t)) + [\Upsilon_\iota(t)] \overline{\varsigma_{\iota\jmath}(t) \beth_\jmath(\hbar \Phi_\jmath(t))} \Big] \leq \sum_{\iota=1}^{n} \sum_{\jmath=1}^{n} |\varsigma_{\iota\jmath}(t) \beth_\jmath(\hbar \Phi_\jmath(t))|_1$$
$$\leq \sum_{\iota=1}^{n} \sum_{\jmath=1}^{n} |\varsigma_{\iota\jmath}(t)|_1 \eta_{1\jmath}. \tag{14}$$

According to Hypothesis 2.2, we can rephrase it as follows:

$$- \frac{1}{2} \sum_{\iota=1}^{n} \sum_{\jmath=1}^{n} \Big[[\overline{\Upsilon_\iota(t)}] \varsigma_{\iota\jmath}(t) \hbar \beth_\jmath(\Phi_\jmath(t)) + [\Upsilon_\iota(t)] \overline{\varsigma_{\iota\jmath}(t) \hbar \beth_\jmath(\Phi_\jmath(t))} \Big]$$
$$\leq - \sum_{\iota=1}^{n} \sum_{\jmath=1}^{n} \Big[\Big(\varsigma_{\iota\jmath}(t) \hbar \beth_\jmath(\Phi_\jmath(t)) \Big)^R sign\Big(\Upsilon_\iota^R(t) \Big) + \Big(\varsigma_{\iota\jmath}(t) \hbar \beth_\jmath(\Phi_\jmath(t)) \Big)^I sign\Big(\Upsilon_\iota^I(t) \Big) \Big]$$
$$\leq \sum_{\iota=1}^{n} \sum_{\jmath=1}^{n} |\varsigma_{\iota\jmath}(t) \hbar \beth_\jmath(\Phi_\jmath(t)|_1 \leq \sum_{\iota=1}^{n} \sum_{\jmath=1}^{n} |\varsigma_{\iota\jmath}(t)|_1 |\hbar|_1 \eta_{1\jmath}. \tag{15}$$

Correspondingly, we have

$$\frac{1}{2} \sum_{\iota=1}^{n} \sum_{\jmath=1}^{n} \Big[[\overline{\Upsilon_\iota(t)}] \sigma_{\iota\jmath}(t) \widehat{\daleth}_\jmath(\Upsilon_\jmath(t - \tau(t))) + [\Upsilon_\iota(t)] \overline{\sigma_{\iota\jmath}(t) \widehat{\daleth}_\jmath(\Upsilon_\jmath(t - \tau(t)))} \Big]$$
$$\leq \sum_{\iota=1}^{n} \sum_{\jmath=1}^{n} |\sigma_{\jmath\iota}(t)|_1 \dot{\daleth}_{1\jmath} |\Upsilon_\iota(t - \tau(t))|_1. \tag{16}$$

$$\frac{1}{2} \sum_{\iota=1}^{n} \sum_{\jmath=1}^{n} \Big[[\overline{\Upsilon_\iota(t)}] \sigma_{\iota\jmath}(t) \daleth_\jmath(\hbar \Phi_\jmath(t - \tau(t))) + [\Upsilon_\iota(t)] \overline{\sigma_{\iota\jmath}(t) \daleth_\jmath(\hbar \Phi_\jmath(t - \tau(t)))} \Big] \leq \sum_{\iota=1}^{n} \sum_{\jmath=1}^{n} |\sigma_{\iota\jmath}(t)|_1 \delta_{1\jmath}. \tag{17}$$

$$\frac{1}{2}\sum_{\iota=1}^{n}\Big[[\overline{\Upsilon_\iota(t)}](1-\hbar)I_\iota(t)+[\Upsilon_\iota(t)]\overline{(1-\hbar)I_\iota(t)}\Big]\leq\sum_{\iota=1}^{n}|1-\hbar|_1\gamma_{1\iota}. \tag{18}$$

And

$$\begin{aligned}&-\frac{1}{2}\sum_{\iota=1}^{n}\sum_{\jmath=1}^{n}\Big[[\overline{\Upsilon_\iota(t)}]\sigma_{\iota\jmath}(t)\hbar\urcorner_\jmath(\Phi_\jmath(t-\tau(t)))+[\Upsilon_\iota(t)]\overline{\sigma_{\iota\jmath}(t)\hbar\urcorner_\jmath(\Phi_\jmath(t-\tau(t)))}\Big]\\&\leq\sum_{\iota=1}^{n}\sum_{\jmath=1}^{n}|\sigma_{\iota\jmath}(t)|_1|\hbar|_1\delta_{1\jmath}.\end{aligned} \tag{19}$$

By calculation

$$-\frac{1}{2}\sum_{\iota=1}^{n}d_\iota\Big[[\overline{\Upsilon_\iota(t)}][\Upsilon_\iota(t)]+[\Upsilon_\iota(t)][\overline{\Upsilon_\iota(t)}]\Big]=-\sum_{\iota=1}^{n}d_\iota[\overline{\Upsilon_\iota(t)}][\Upsilon_\iota(t)]\leq-\sum_{\iota=1}^{n}d_\iota. \tag{20}$$

When incorporating inequalities (12) to (20) into inequality (11), we obtain

$$\begin{aligned}&{}_{t_0}D_t^{\kappa}\mathbb{V}_1(t)\\&\leq-\sum_{\iota=1}^{n}(o_\iota+c_\iota)|\Upsilon_\iota(t)|_1+\sum_{\iota=1}^{n}\sum_{\jmath=1}^{n}|\varsigma_{\jmath\iota}(t)|_1\dot{\urcorner}_{\jmath1}|\Upsilon_\iota(t)|_1\\&\quad+\sum_{\iota=1}^{n}\sum_{\jmath=1}^{n}|\sigma_{\jmath\iota}(t)|_1\dot{\urcorner}_{1\jmath}|\Upsilon_\iota(t-\tau(t))|_1+|1-\hbar|_1\sum_{\iota=1}^{n}\gamma_{1\iota}\\&\quad+(1+|\hbar|_1)\sum_{\iota=1}^{n}\sum_{\jmath=1}^{n}\Big(|\varsigma_{\iota\jmath}(t)|_1\eta_{1\jmath}+|\sigma_{\iota\jmath}(t)|_1\delta_{1\jmath}\Big)-d_\iota\\&\leq-(\mathfrak{I}-\mathfrak{R}_1)\sum_{\iota=1}^{n}|\Upsilon_\iota(t)|_1+\mathfrak{R}_2\sum_{\iota=1}^{n}|\Upsilon_\iota(t-\tau(t))|_1+\varrho.\end{aligned} \tag{21}$$

For $\wp>1$, according to the fractional-order Razumikhin theorem [35], it is affirmed that

$${}_{t_0}D_t^{\kappa}\mathbb{V}_1(t)\leq-(\mathfrak{I}-\mathfrak{R}_1-\wp\mathfrak{R}_2)\mathbb{V}_1(t)+\varrho=-\mathfrak{R}\mathbb{V}_1(t)+\varrho. \tag{22}$$

Referring to Lemma 2.5, we have

$$\mathbb{V}_1(t)\leq\Big(\mathbb{V}_1(t_0)-\frac{\varrho}{\mathfrak{R}}\Big)E_\kappa(-\mathfrak{R}t^{\kappa})+\frac{\varrho}{\mathfrak{R}}. \tag{23}$$

That is

$$\|\Upsilon_\iota(t)\|_1\leq\Big(\|\Upsilon_\iota(t_0)\|_1-\frac{\varrho}{\mathfrak{R}}\Big)E_\kappa(-\mathfrak{R}t^{\kappa})+\frac{\varrho}{\mathfrak{R}}. \tag{24}$$

According to Lemma 2.6, it implies

$$\lim_{t\to\infty}\|\Upsilon_\iota(t)\|_1\leq\frac{\varrho}{\mathfrak{R}}. \tag{25}$$

Hence, FOMCVDNNS (3) is QTS with FOMCVDNNs (2) under the hybrid controller (4), the proof has been completed.

Remark 3.1. The inclusion of $d_\iota[\Upsilon_\iota(t)]$ in the controller (4) serves the purpose of adjusting ϱ, allowing for manual control of the error $\frac{\varrho}{\Re}$. Ensuring that $\Upsilon_\iota(t) \neq 0$ is imperative, as any deviation from this condition would lead to the establishment of a stable error system. This crucial stipulation validates the inequality (20).

3.2. Finite-time synchronization

Taking $\Xi_\iota(t) = \Psi_\iota(t) - \Phi_\iota(t)$ and incorporating FOMCVDNNs (2) and (3), we can express the error system as follows:

$$\begin{aligned} {}_{t_0}D_t^{\kappa}\Xi_\iota(t) = &- o_\iota\Xi_\iota(t) + \sum_{\iota=1}^{n} \varsigma_{\iota\jmath}(\Psi_\iota(t))\beth_\jmath(\Psi_\jmath(t)) - \sum_{\jmath=1}^{n} \varsigma_{\iota\jmath}(\Phi_\iota(t))\beth_\jmath(\Phi_\jmath(t)) \\ &+ \sum_{\jmath=1}^{n} \sigma_{\iota\jmath}(\Psi_\iota(t))\daleth_\jmath(\Psi_\jmath(t-\tau(t))) - \sum_{\jmath=1}^{n} \sigma_{\iota\jmath}(\Phi_\iota(t))\daleth_\jmath(\Phi_\jmath(t-\tau(t))) + u_\iota(t). \end{aligned} \tag{26}$$

To achieve FNTS for both FOMCVDNNs (2) and (3), we propose the implementation of a hybrid controller through the following design:

$$u_\iota(t) = -[\Xi_\iota(t)](\psi_\iota|\Xi_\iota(t)|_1^{\zeta}) - \theta_\iota\Xi_\iota(t) - \widetilde{\nu}_\iota(t), \tag{27}$$

where $\psi_\iota > 0$, $0 < \zeta < \kappa < 1$ and $\theta_\iota > 0$. $\widetilde{\nu}_\iota(t)$ is designed as:

$$\widetilde{\nu}_\iota(t) = \begin{cases} 0, |\Phi_\iota(t)|_1 \leq \Omega_\iota, |\Psi_\iota(t)|_1 \leq \Omega_\iota, \\ 0, |\Phi_\iota(t)|_1 > \Omega_\iota, |\Psi_\iota(t)|_1 > \Omega_\iota, \\ \sum\limits_{\jmath=1}^{n} \Big[(\varsigma_{\iota\jmath}^{**} - \varsigma_{\iota\jmath}^{*})\beth_\jmath(\Phi_\jmath(t)) + (\sigma_{\iota\jmath}^{**} - \sigma_{\iota\jmath}^{*}) \times \daleth_\jmath(\Phi_\jmath(t-\tau(t)))\Big], |\Phi_\iota(t)|_1 \leq \Omega_\iota, |\Psi_\iota(t)|_1 > \Omega_\iota, \\ \sum\limits_{\jmath=1}^{n} \Big[(\varsigma_{\iota\jmath}^{*} - \varsigma_{\iota\jmath}^{**})\beth_\jmath(\Phi_\jmath(t)) + (\sigma_{\iota\jmath}^{*} - \sigma_{\iota\jmath}^{**}) \times \daleth_\jmath(\Phi_\jmath(t-\tau(t)))\Big], |\Phi_\iota(t)|_1 > \Omega_\iota, |\Psi_\iota(t)|_1 \leq \Omega_\iota. \end{cases} \tag{28}$$

Under the hybrid controller (27), the error system (26) can be covered with the following differential inclusions

$$\begin{aligned} {}_{t_0}D_t^{\kappa}\Xi_\iota(t) \in &- (o_\iota + \theta_\iota)\Xi_\iota(t) + \sum_{\jmath=1}^{n} \overline{co}[\varsigma_{\iota\jmath}^{*}, \varsigma_{\iota\jmath}^{**}]\widetilde{\beth}_\jmath(\Xi_\jmath(t)) \\ &+ \sum_{\jmath=1}^{n} \overline{co}[\sigma_{\iota\jmath}^{*}, \sigma_{\iota\jmath}^{**}]\widetilde{\daleth}_\jmath(\Xi_\jmath(t-\tau(t))) - [\Xi_\iota(t)](\psi_\iota|\Xi_\iota(t)|_1^{\zeta}). \end{aligned} \tag{29}$$

Through the application of the measurable selection theorem [32, 33] and the lemma 2.1 of [34], function $\varsigma_{\iota\jmath}(t) \in \overline{co}[\varsigma_{\iota\jmath}^{*}, \varsigma_{\iota\jmath}^{**}]$ and $\sigma_{\iota\jmath}(t) \in \overline{co}[\sigma_{\iota\jmath}^{*}, \sigma_{\iota\jmath}^{**}]$, $\varpi_\iota(t) \in \overline{co}[\Xi_\iota(t)]$ can be found such that

$${}_{t_0}D_t^{\kappa}\Xi_\iota(t) = -(o_\iota + \theta_\iota)\Xi_\iota(t) + \sum_{\jmath=1}^{n} \varsigma_{\iota\jmath}(t)\widetilde{\beth}_\jmath(\Xi_\jmath(t)) + \sum_{\jmath=1}^{n} \sigma_{\iota\jmath}(t)\widetilde{\daleth}_\jmath(\Xi_\jmath(t-\tau(t))) - \varpi_\iota(t)(\psi_\iota|\Xi_\iota(t)|_1^{\zeta}). \tag{30}$$

where $\widetilde{\jmath}_j(\Xi_j(t)) = \jmath_j(\Psi_j(t)) - \jmath_j(\Phi_j(t))$, $\widetilde{\urcorner}_j(\Xi_j(t-\tau(t))) = \urcorner_j(\Psi_j(t-\tau(t))) - \urcorner_j(\Phi_j(t-\tau(t)))$.

Theorem 3.2. Based on Hypotheses 2.1 and 2.2, the FOMCVDNNs (2) and (3) get FNTS under controller (27) if

$$\mathfrak{R}^{\diamond} = \mathfrak{I}^{\diamond} - \mathfrak{R}_1^{\diamond} - \wp^{\diamond}\mathfrak{R}_2^{\diamond} > 0, \tag{31}$$

where

$$\mathfrak{I}^{\diamond} = \min_{\iota\in\mathbb{Q}}\{o_\iota + \theta_\iota\}, \quad \mathfrak{R}_1^{\diamond} = \max_{\iota\in\mathbb{Q}}\{\sum_{j=1}^{n} \dot{\jmath}_{j1}|\varsigma_{\iota j}|_1\}, \quad \mathfrak{R}_2^{\diamond} = \max_{\iota\in\mathbb{Q}}\{\sum_{j=1}^{n} \dot{\urcorner}_{j1}|\sigma_{\iota j}|_1\}, \quad \wp^{\diamond} > 1.$$

Proof. Constructing the designated Lyapunov function as outlined:

$$\mathbb{V}_2(t) = \sum_{\iota=1}^{n} |\Xi_\iota(t)|_1.$$

Based on Lemma 2.1, one has

$$\begin{aligned}
&{}_{t_0}D_t^{\kappa}\mathbb{V}_2(t)\\
\leq&\frac{1}{2}\sum_{\iota=1}^{n}\Big[[\overline{\Xi_p(t)}]_{t_0}D_t^{\kappa}\Xi_\iota(t) + [\Xi_p(t)]_{t_0}D_t^{\kappa}\overline{\Xi_\iota(t)}\Big]\\
=&-\frac{1}{2}\sum_{\iota=1}^{n}(o_\iota+\theta_\iota)\Big[\Xi_\iota(t)[\overline{\Xi_\iota(t)}] + \overline{\Xi_\iota(t)}[\Xi_\iota(t)]\Big]\\
&+\frac{1}{2}\sum_{\iota=1}^{n}\sum_{j=1}^{n}\Big[[\overline{\Xi_\iota(t)}]\varsigma_{\iota j}(t)\widetilde{\jmath}_j(\Xi_j(t)) + [\Xi_\iota(t)]\overline{\varsigma_{\iota j}(t)\widetilde{\jmath}_j(\Xi_j(t))}\Big]\\
&+\frac{1}{2}\sum_{\iota=1}^{n}\sum_{j=1}^{n}\Big[[\overline{\Xi_\iota(t)}]\sigma_{\iota j}(t)\widetilde{\urcorner}_j(\Xi_j(t-\tau(t))) + [\Xi_\iota(t)]\overline{\sigma_{\iota j}(t)\widetilde{\urcorner}_j(\Xi_j(t-\tau(t)))}\Big]\\
&-\frac{1}{2}\sum_{\iota=1}^{n}\psi_\iota\Big[[\Xi_\iota(t)]\overline{\varpi_\iota(t)} + [\overline{\Xi_\iota(t)}]\varpi_\iota(t)\Big]|\Xi_\iota(t)|_1^{\zeta}.
\end{aligned}\tag{32}$$

By utilizing Lemmas 2.2 and 2.3, we can rephrase this as

$$-\frac{1}{2}\sum_{\iota=1}^{n}\psi_\iota\Big[[\Xi_\iota(t)]\overline{\varpi_\iota(t)} + [\overline{\Xi_\iota(t)}]\varpi_\iota(t)\Big]|\Xi_\iota(t)|_1^{\zeta} = -\sum_{\iota=1}^{n}\psi_\iota|[\Xi_\iota(t)]|_1|\Xi_\iota(t)|_1^{\zeta} \leq -\psi_\iota\Big(\sum_{\iota=1}^{n}|\Xi_\iota(t)|_1\Big)^{\zeta}. \tag{33}$$

Correspondingly, using the formula of inequality (33) and Theorem 3.1 to represent inequality (32), we can infer

$$\begin{aligned}
{}_{t_0}D_t^{\kappa}\mathbb{V}_2(t) \leq&-\sum_{\iota=1}^{n}(o_\iota+\theta_\iota)|\Xi_\iota(t)|_1 + \sum_{\iota=1}^{n}\sum_{j=1}^{n}\dot{\jmath}_{j1}|\varsigma_{\iota j}|_1|\Xi_\iota(t)|_1\\
&+\sum_{\iota=1}^{n}\sum_{j=1}^{n}\dot{\urcorner}_{j1}|\sigma_{\iota j}|_1|\Xi_j(t-\tau(t))|_1 - \psi_\iota\Big(\sum_{\iota=1}^{n}|\Xi_\iota(t)|_1\Big)^{\zeta}.
\end{aligned}\tag{34}$$

For $\wp^{\diamond} > 1$, according to the fractional-order Razumikhin theorem [35], it holds that

$$ {}_{t_0}D_t^{\kappa}\mathbb{V}_2(t) \leq -(\mathfrak{J}^{\diamond} - \mathfrak{R}_1^{\diamond} - \wp^{\diamond}\mathfrak{R}_2^{\diamond})\mathbb{V}_2(t) - \psi_{\iota}\mathbb{V}_2(t)^{\zeta}. \tag{35} $$

According to $\mathfrak{J}^{\diamond} - \mathfrak{R}_1^{\diamond} - \wp^{\diamond}\mathfrak{R}_2^{\diamond} > 0$ in Theorem 3.2, we obtain

$$ {}_{t_0}D_t^{\kappa}\mathbb{V}_2(t) \leq -\psi_{\iota}\mathbb{V}_2(t)^{\zeta}. \tag{36} $$

In Lemma 2.4, it is demonstrated that FOMCVDNNs(2) and (3), when operating under the hybrid controller (27), can achieve synchronization within the given time frame T. This completes the proof for Theorem 3.2.

Remark 3.2. We introduce the utilization of the complex-valued sign function for investigating QPS and FNTS in FOMCVDNNs through a non-separation method. In contrast to traditional methods that entail the division of complex-valued systems into two distinct real-valued systems [20–23], our research showcases a notable decrease in conservatism and computational complexity. This novel approach not only enhances the range of application but also augments the generality of our research outcomes.

Remark 3.3. In contrast to linear feedback control schemes [36, 37], the distinctive features of fractional-order complex-valued neural networks align effectively with the capabilities of hybrid control. This alignment renders hybrid control particularly well-suited for addressing the intricacies inherent in such systems. Furthermore, the hybrid control approach can contribute to increased stability, ensuring that the synchronized state is maintained even in the presence of disturbances or uncertainties.

4. Numerical example

In this segment, we will conduct a numerical simulation to demonstrate the soundness of the suggested outcomes.

Example 4.1. Consider a class of 2-dimensional FOMCVDNNs

$$ {}_{t_0}D_t^{\kappa}\Phi_{\iota}(t) = -o_{\iota}\Phi_{\iota}(t) + \sum_{j=1}^{n} \varsigma_{\iota j}(\Phi_{\iota}(t))\beth_j(\Phi_j(t)) + \sum_{j=1}^{n} \sigma_{\iota j}(\Phi_{\iota}(t))\urcorner_j(\Phi_j(t-\tau(t))) + I_{\iota}(t), \tag{37} $$

in which

$$ \varsigma_{11}(\Phi_1(t)) = \begin{cases} -1 - 0.5\mathbf{i}, & |\Phi_1(t)|_1 \leq 1 \\ -1 - \mathbf{i}, & |\Phi_1(t)|_1 > 1 \end{cases} \quad \varsigma_{12}(\Phi_1(t)) = \begin{cases} 0.7 - 0.8\mathbf{i}, & |\Phi_1(t)|_1 \leq 1 \\ 0.3 - \mathbf{i}, & |\Phi_1(t)|_1 > 1 \end{cases} $$

$$ \varsigma_{21}(\Phi_2(t)) = \begin{cases} 0.3 - 0.6\mathbf{i}, & |\Phi_2(t)|_1 \leq 1 \\ 1 - 0.5\mathbf{i}, & |\Phi_2(t)|_1 > 1 \end{cases} \quad \varsigma_{22}(\Phi_2(t)) = \begin{cases} 1 - \mathbf{i}, & |\Phi_2(t)|_1 \leq 1 \\ 0.6 - 0.3\mathbf{i}, & |\Phi_2(t)|_1 > 1 \end{cases} $$

$$ \sigma_{11}(\Phi_1(t)) = \begin{cases} -0.5 - 0.2\mathbf{i}, & |\Phi_1(t)|_1 \leq 1 \\ -0.2 - 0.8\mathbf{i}, & |\Phi_1(t)|_1 > 1 \end{cases} \quad \sigma_{12}(\Phi_1(t)) = \begin{cases} 0.5 + 0.1\mathbf{i}, & |\Phi_1(t)|_1 \leq 1 \\ -0.2 - 0.2\mathbf{i}, & |\Phi_1(t)|_1 > 1 \end{cases} $$

$$ \sigma_{21}(\Phi_2(t)) = \begin{cases} 0.5 - 0.5\mathbf{i}, & |\Phi_2(t)|_1 \leq 1 \\ -0.8\mathbf{i}, & |\Phi_2(t)|_1 > 1 \end{cases} \quad \sigma_{22}(\Phi_2(t)) = \begin{cases} -0.5\mathbf{i}, & |\Phi_2(t)|_1 \leq 1 \\ -0.5 - \mathbf{i}, & |\Phi_2(t)|_1 > 1 \end{cases} $$

and $\kappa = 0.98$, $\beth_j(\Phi_j(t)) = \daleth_j(\Phi_j(t)) = tanh(Re(\Phi_j(t))) + \mathbf{i}tanh(Im(\Phi_j(t)))$, $O = diag(o_1, o_2) = diag(1, 1)$, $\tau(t) = \frac{e^t}{1+e^t}$, $I_\iota = (\mathbf{i}, -\mathbf{i})^T$, the initial value of system (37) is $\dagger(0) = (-0.4 + 0.6\mathbf{i}, 1.1 + 0.5\mathbf{i})^T$.

The corresponding response system is denoted by

$$ {}_{t_0}D_t^{\kappa}\Psi_\iota(t) = -o_\iota\Psi_\iota(t) + \sum_{j=1}^{n} \varsigma_{\iota j}(\Psi_\iota(t))\beth_j(\Psi_j(t)) + \sum_{j=1}^{n} \sigma_{\iota j}(\Psi_\iota(t))\daleth_j(\Psi_j(t-\tau(t))) + I_\iota(t) + u_\iota(t), \tag{38} $$

where $o_\iota, \varsigma_{\iota j}(\Psi_\iota(t)), \sigma_{\iota j}(\Psi_\iota(t)), \beth_j(\Psi_\iota(t)), \daleth_j(\Psi_\iota(t)), \tau(t), I_\iota(t)$ are the same as in system (37). The initial value of system (38) is $\ddagger(0) = (-1.1 - 0.4\mathbf{i}, 1.4 - \mathbf{i})$.

The graph of FOMCVDNNs (37) is divided into real and image parts. The phase plot of $Re(\Phi_1(t))$, $Re(\Phi_2(t))$, $Im(\Phi_1(t))$, $Im(\Phi_2(t))$ are given in Figure 1. The state trajectory of the real and image parts of FOMCVDNNs (37) are given in Figure 2.

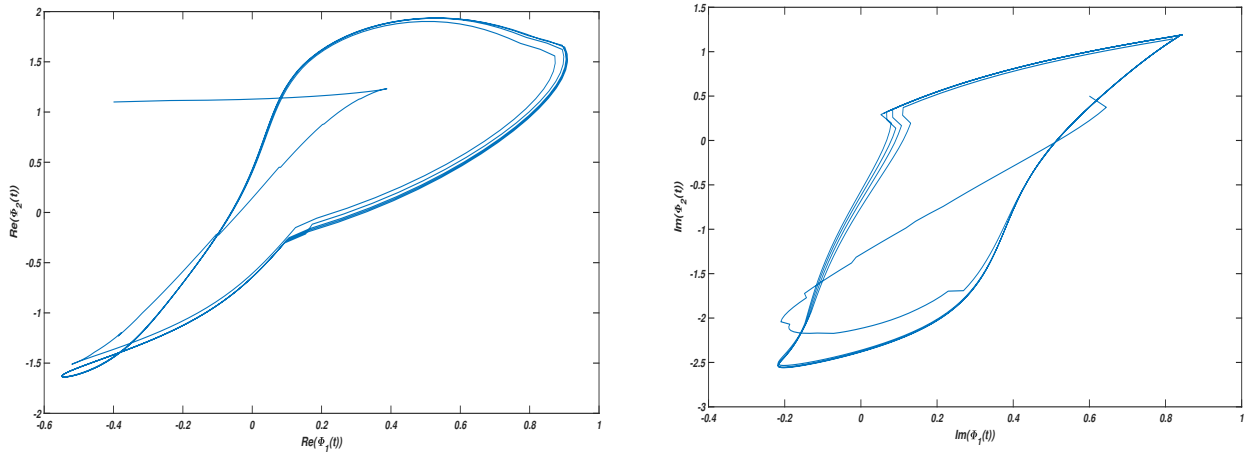

Figure 1. State variable phase diagram for system (37).

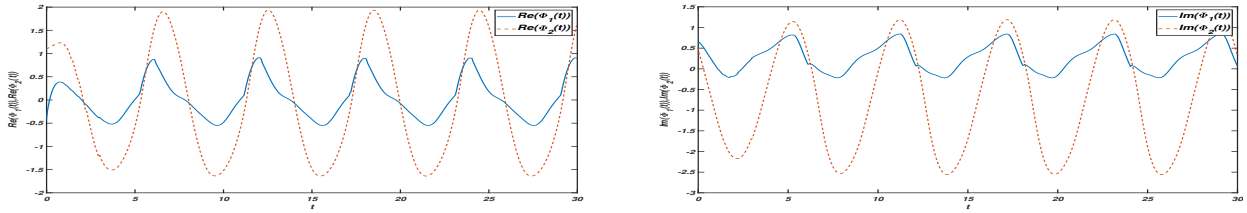

Figure 2. State trajectory of real and imag part of system (37) without control.

First, the feasibility of Theorem 3.1 is verified. Choose $\hbar = 0.5$, $\beth_{1j} = \daleth_{1j} = 1$, $\eta_{1j} = \delta_{1j} = 2$, $\varphi_{11} = \varphi_{12} = 1$, $c_1 = c_2 = 35$, $d_1 = d_2 = 20$. By calculation, $\Im = 1 + 35 = 36$, $\Re_1 = max\{\sum_{j=1}^{2} \beth_{11}|\varsigma_{j1}|_1, \sum_{j=1}^{2} \beth_{12}|\varsigma_{j2}|_1\} = max\{3.5, 3.5\} = 3.5$, $\Re_2 = max\{\sum_{j=1}^{2} \daleth_{11}|\sigma_{j1}|_1, \sum_{j=1}^{2} \daleth_{12}|\sigma_{j2}|_1\} = max\{2, 2.1\} = 2.1$, $\varrho = 14.3$, For $\wp = 1.1$, we have $\Re_1 + \wp\Re_2 = 5.81$, $\Re = \Im - \Re_1 - \wp\Re_2 = 30.19$. Thus, we can get error bound $\frac{\varrho}{\Re} \approx 0.474$. Therefore, system (37) is QTS with system (38) under the controller (4). Figure 3 shows the time responses of state variables $\hbar\Phi_\iota(t)$ and $\Psi_\iota(t)$ under $\hbar = 0.5$ and controller (4). Figure 4 shows time responses of synchronization error $\Upsilon_\iota(t)$ with hybrid controller (4), and the error bound is clearly within the range of 0.474.

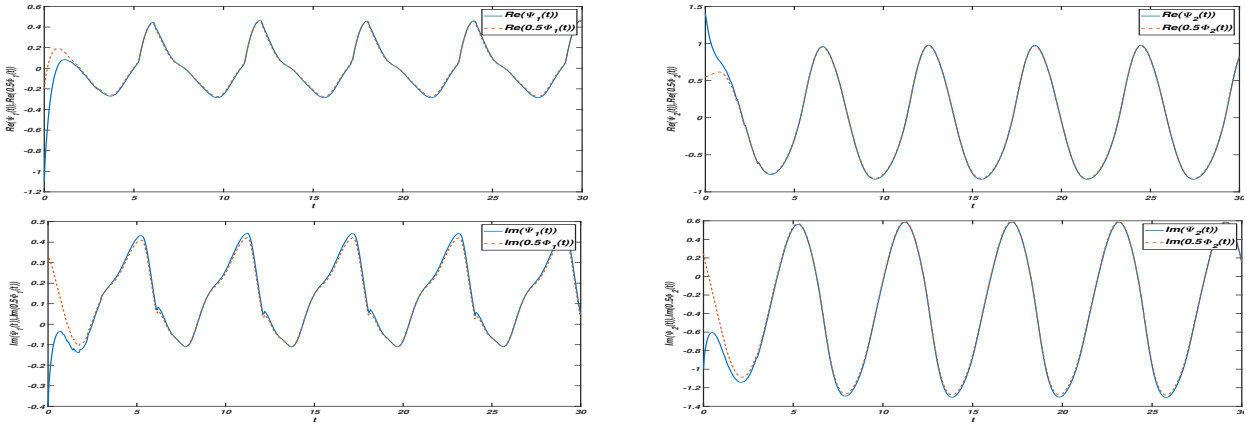

Figure 3. Time responses of state variables $\hbar\Phi_\iota(t)$ and $\Psi_\iota(t)$ under $\hbar = 0.5$ and hybrid controller (4).

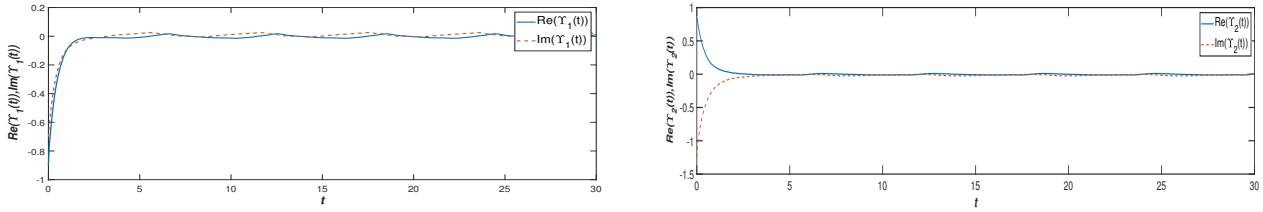

Figure 4. Time responses of synchronization error $\Upsilon_\iota(t)$ with hybrid controller (4).

In control protocol (27), we choose $\psi_\iota = 1.25$, $\zeta = 0.9$ and $\theta_\iota = 2$. $I_1 = I_2 = 0$. To enhance convenience, we opt for identical system parameters, initial conditions, and fractional order. According to Theorem 3.2, we know that FOMCVDNNs (37) and (38) can achieve FNTS based on the hybrid controller (27). The settling time can be approximated as $T = 9.053$. Figure 5 shows the synchronization error of $\Xi_\iota(t)$ with controller (27). Synchronization of $\Phi_1(t), \Psi_1(t)$ and $\Phi_2(t), \Psi_2(t)$ with controller (27) is shown in Figure 6.

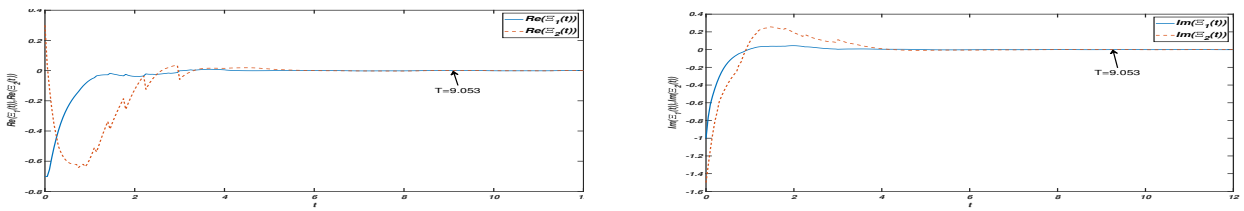

Figure 5. Time responses of synchronization error $\Xi_\iota(t)$ with hybrid controller (27).

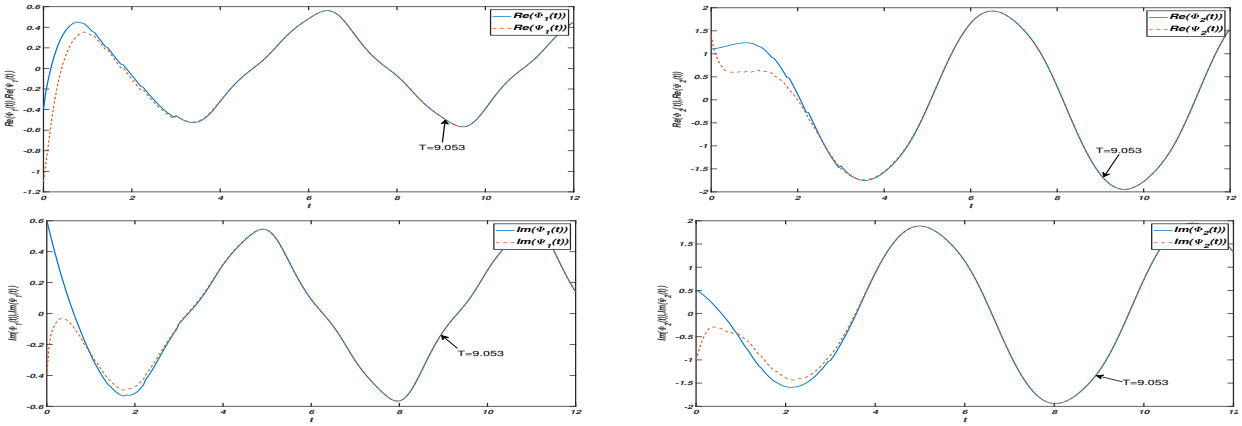

Figure 6. Synchronization of $\Phi_t(t)$ and $\Psi_t(t)$ with hybrid controller (27).

Remark 4.1. Choosing a fractional order close to an integer (e.g., 0.98) may provide a smoother transition from the well-established integer-order control methods to fractional-order methods. This helps in leveraging the benefits of fractional calculus while maintaining a level of familiarity with traditional control concepts.

5. Conclusions

We investigated the QPS and FNTS for FOMCVDNNs. Employing non-separation methods, we directly examined the FOMCVDNNs and derived the necessary criteria for QPS and FNTS using the hybrid control scheme. The results presented in this article enrich the synchronization control findings of pre-existing FOMCVDNNs [38, 39]. Finally, through numerical simulation, the theoretical results were substantiated. In our future research, we consider incorporating distributed delay into the system and investigate its fixed-time, preassigned-time, and discrete-time [40] synchronization problems.

Use of AI tools declaration

The authors declare they have not used Artificial Intelligence (AI) tools in the creation of this article.

Acknowledgments

The authors thank the reviewer for their careful reading and suggestions. This work is supported by the National Science Foundation of China Nos. 61976228 and 62076106.

Conflict of interest

The authors declare that they have no conflicts of interest.

References

1. W. Xu, J. Cao, M. Xiao, D. W. Ho, G. Wen, A new framework for analysis on stability and bifurcation in a class of neural networks with discrete and distributed delays, *IEEE Trans. Cybern.*, **45** (2015), 2224–2236. https://doi.org/10.1109/TCYB.2014.2367591

2. L. Wang, T. Dong, M. F. Ge, Finite-time synchronization of memristor chaotic systems and its application in image encryption, *Appl. Math. Comput.*, **347** (2019), 293–305. https://doi.org/10.1016/j.amc.2018.11.017

3. F. C. Hoppensteadt, E. M. Izhikevich, Pattern recognition via synchronization in phase-locked loop neural networks, *IEEE Trans. Neural Netw.*, **11** (2000), 734–738. https://doi.org/10.1109/72.846744

4. H. Shen, Y. Zhu, L. Zhang, J. H. Park, Extended dissipative state estimation for markov jump neural networks with unreliable links, *IEEE Trans. Neural Netw. Learn. Syst.*, **28** (2016), 346–358. https://doi.org/10.1109/TNNLS.2015.2511196

5. C. Xu, M. Liao, P. Li, Y. Guo, Q. Xiao, S. Yuan, Influence of multiple time delays on bifurcation of fractional-order neural networks, *Appl. Math. Comput.*, **361** (2019), 565–582. https://doi.org/10.1016/j.amc.2019.05.057

6. P. Liu, Z. Zeng, J. Wang, Asymptotic and finite-time cluster synchronization of coupled fractional-order neural networks with time delay, *IEEE Trans. Neural Netw. Learn. Syst.*, **31** (2020), 4956–4967. https://doi.org/10.1109/TNNLS.2019.2962006

7. A. Pratap, R. Raja, J. Alzabut, J. Cao, G. Rajchakit, C. Huang, Mittag-leffler stability and adaptive impulsive synchronization of fractional order neural networks in quaternion field, *Math. Methods Appl. Sci.*, **43** (2020), 6223–6253. https://doi.org/10.1002/mma.6367

8. L. Chua, Memristor-the missing circuit element, *IEEE Trans. Circuit Theory*, **18** (1971), 507–519. https://doi.org/10.1109/TCT.1971.1083337

9. J. Zhou, X. Ma, Z. Yan, S. Arik, Non-fragile output-feedback control for time-delay neural networks with persistent dwell time switching: A system mode and time scheduler dual-dependent design, *Neural Netw.*, **169** (2024), 733–743. https://doi.org/10.1016/j.neunet.2023.11.007

10. J. W. Smith, Complex-valued neural networks for data-driven signal processing and signal understanding, *arXiv:2309.07948*, 2023. https://doi.org/10.48550/arXiv.2309.07948

11. R. Trabelsi, I. Jabri, F. Melgani, F. Smach, N. Conci, A. Bouallegue, Indoor object recognition in rgbd images with complex-valued neural networks for visually-impaired people, *Neurocomputing*, **330** (2019), 94–103. https://doi.org/10.1016/j.neucom.2018.11.032

12. M. Z. Khan, A. Sarkar, A. Noorwali, Memristive hyperchaotic system-based complex-valued artificial neural synchronization for secured communication in industrial internet of things, *Eng. Appl. Artif. Intell.*, **123** (2023), 106357. https://doi.org/10.1016/j.engappai.2023.106357

13. H. Zhang, J. Cheng, H. Zhang, W. Zhang, J. Cao, Quasi-uniform synchronization of caputo type fractional neural networks with leakage and discrete delays, *Chaos Solitons Fractals*, **152** (2021), 111432. https://doi.org/10.1016/j.chaos.2021.111432

14. S. Yang, J. Yu, C. Hu, H. Jiang, Quasi-projective synchronization of fractional-order complex-valued recurrent neural networks, *Neural Netw.*, **104** (2018), 104–113. https://doi.org/10.1016/j.neunet.2018.04.007

15. H. Zhang, Y. Cheng, H. Zhang, W. Zhang, J. Cao, Hybrid control design for mittag-leffler projective synchronization on foqvnns with multiple mixed delays and impulsive effects, *Math. Comput. Simul.*, **197** (2022), 341–357. https://doi.org/10.1016/j.matcom.2022.02.022

16. H. L. Li, J. Cao, H. Jiang, A. Alsaedi, Finite-time synchronization of fractional-order complex networks via hybrid feedback control, *Neurocomputing*, **320** (2018), 69–75. https://doi.org/10.1016/j.neucom.2018.09.021
17. H. L. Li, J. Cao, H. Jiang, A. Alsaedi, Finite-time synchronization and parameter identification of uncertain fractional-order complex networks, *Physica A*, **533** (2019), 122027. https://doi.org/10.1016/j.physa.2019.122027
18. H. Yan, Y. Qiao, L. Duan, J. Miao, New results of quasi-projective synchronization for fractional-order complex-valued neural networks with leakage and discrete delays, *Chaos Solitons Fractals*, **159** (2022), 112121. https://doi.org/10.1016/j.chaos.2022.112121
19. H. L. Li, C. Hu, J. Cao, H. Jiang, A. Alsaedi, Quasi-projective and complete synchronization of fractional-order complex-valued neural networks with time delays, *Neural Netw.*, **118** (2019), 102–109. https://doi.org/10.1016/j.neunet.2019.06.008
20. X. Li, X. Liu, F. Wang, Anti-synchronization of fractional-order complex-valued neural networks with a leakage delay and time-varying delays, *Chaos Solitons Fractals*, **174** (2023), 113754. https://doi.org/10.1016/j.chaos.2023.113754
21. Y. Cheng, T. Hu, W. Xu, X. Zhang, S. Zhong, Fixed-time synchronization of fractional-order complex-valued neural networks with time-varying delay via sliding mode control, *Neurocomputing*, **505** (2022), 339–352. https://doi.org/10.1016/j.neucom.2022.07.015
22. X. Song, X. Sun, J. Man, S. Song, Q. Wu, Synchronization of fractional-order spatiotemporal complex-valued neural networks in finite-time interval and its application, *J. Franklin Inst.*, **358** (2021), 8207–8225. https://doi.org/10.1016/j.jfranklin.2021.08.016
23. K. Udhayakumar, R. Rakkiyappan, F. A. Rihan, S. Banerjee, Projective multi-synchronization of fractional-order complex-valued coupled multi-stable neural networks with impulsive control, *Neurocomputing*, **467** (2022), 392–405. https://doi.org/10.1016/j.neucom.2021.10.003
24. J. Yang, H. L. Li, L. Zhang, C. Hu, H. Jiang, Quasi-projective and finite-time synchronization of delayed fractional-order bam neural networks via quantized control, *Math. Methods Appl. Sci.*, **46** (2023), 197–214. https://doi.org/10.1002/mma.8504
25. N. Yao, M. Hui, J. Zhang, J. Yan, W. Wu, Complete synchronization of delayed fractional-order complex-valued neural networks via adaptive control, In: *2022 5th International conference on artificial intelligence and big data*, 2022, 173–178. https://doi.org/10.1109/ICAIBD55127.2022.9820317
26. A. A. Kilbas, H. M. Srivastava, J. J. Trujillo, *Theory and applications of fractional differential equations*, New York: Elsevier, 2006.
27. X. Yang, J. Cao, Finite-time stochastic synchronization of complex networks, *Appl. Math. Model.*, **34** (2010), 3631–3641. https://doi.org/10.1016/j.apm.2010.03.012
28. L. Feng, J. Yu, C. Hu, C. Yang, H. Jiang, Nonseparation method-based finite/fixed-time synchronization of fully complex-valued discontinuous neural networks, *IEEE Trans. Cybern.*, **51** (2020), 3212–3223. https://doi.org/10.1109/TCYB.2020.2980684
29. Q. Gan, L. Li, J. Yang, Y. Qin, M. Meng, Improved results on fixed-/preassigned-time synchronization for memristive complex-valued neural networks, *IEEE Trans. Neural Netw. Learn. Syst.*, **33** (2021), 5542–5556. https://doi.org/10.1109/TNNLS.2021.3070966

30. B. Zheng, C. Hu, J. Yu, H. Jiang, Finite-time synchronization of fully complex-valued neural networks with fractional-order, *Neurocomputing*, **373** (2020), 70–80. https://doi.org/10.1016/j.neucom.2019.09.048

31. A. A. Kilbas, M. Saigo, R. K. Saxena, Generalized mittag-leffler function and generalized fractional calculus operators, *Integral Transform. Spec. Funct.*, **15** (2004), 31–49. https://doi.org/10.1080/10652460310001600717

32. J. P. Aubin, A. Cellina, *Differential inclusions: Set-valued maps and viability theory*, Berlin, Heidelberg: Springer, 2012. https://doi.org/10.1007/978-3-642-69512-4

33. A. F. Filippov, *Differential equations with discontinuous righthand sides: Control systems*, Dordrecht: Springer, 2013. https://doi.org/10.1007/978-94-015-7793-9

34. G. Zhang, Z. Zeng, D. Ning, Novel results on synchronization for a class of switched inertial neural networks with distributed delays, *Inf. Sci.*, **511** (2020), 114–126. https://doi.org/10.1016/j.ins.2019.09.048

35. D. Baleanu, S. Sadati, R. Ghaderi, A. Ranjbar, T. Abdeljawad, F. Jarad, Razumikhin stability theorem for fractional systems with delay, *Abstr. Appl. Anal.*, **2010** (2010), 124812. https://doi.org/10.1155/2010/124812

36. J. Jia, Z. Zeng, Lmi-based criterion for global mittag-leffler lag quasi-synchronization of fractional-order memristor-based neural networks via linear feedback pinning control, *Neurocomputing*, **412** (2020), 226–243. https://doi.org/10.1016/j.neucom.2020.05.074

37. Y. Fan, X. Huang, Z. Wang, Y. Li, Improved quasi-synchronization criteria for delayed fractional-order memristor-based neural networks via linear feedback control, *Neurocomputing*, **306** (2018), 68–79. https://doi.org/10.1016/j.neucom.2018.03.060

38. Y. Shen, S. Zhu, X. Liu, S. Wen, Multiple mittag-leffler stability of fractional-order complex-valued memristive neural networks with delays, *IEEE Trans. Cybern.*, **53** (2022), 5815–5825. https://doi.org/10.1109/TCYB.2022.3194059

39. M. Syed Ali, G. Narayanan, Z. Orman, V. Shekher, S. Arik, Finite time stability analysis of fractional-order complex-valued memristive neural networks with proportional delays, *Neural Process. Lett.*, **51** (2020), 407–426. https://doi.org/10.1007/s11063-019-10097-7

40. J. Zhou, J. Dong, S. Xu, Asynchronous dissipative control of discrete-time fuzzy markov jump systems with dynamic state and input quantization, *IEEE Trans. Fuzzy Syst.*, **31** (2023), 3906–3920. https://doi.org/10.1109/TFUZZ.2023.3271348

AIMS Press